Elimination of a zero-order beam induced by a pixelated spatial light modulator for holographic projection

Hao Zhang, Jinghui Xie, Juan Liu,* and Yongtian Wang

Department of Photo-electric Engineering, School of Information Science and Technology, Beijing Institute of Technology, Beijing 100081, China

*Corresponding author: juanliu@bit.edu.cn

Received 9 June 2009; revised 3 September 2009; accepted 30 September 2009; posted 1 October 2009 (Doc. ID 112573); published 16 October 2009

A technique is proposed theoretically and verified experimentally to eliminate a zero-order beam caused by a pixelated phase-only spatial light modulator (SLM) for holographic projection. The formulas for determination of the optical field in the Fourier plane are deduced, and the influence of the pixelated structure of a SLM on the intensity of the zero-order beam is numerically investigated. Two currently existing techniques are studied and a new one is presented. These three techniques are used separately to eliminate the zero-order interruption, and the optical performances of the reconstructed patterns are compared. The new technique results in higher reconstruction quality and diffraction efficiency. A short animated movie is illuminated for holographic projection display. The experimental results show that the zero-order beam can be efficiently eliminated by the new technique. It is believed that this technique can be used in various optical systems that are based on pixelated phase-only SLMs, such as holographic optical tweezers and optical testing systems. © 2009 Optical Society of America

OCIS codes: 090.1760, 090.2870.

1. Introduction

Phase-only holograms can project two-dimensional images based on diffraction theory. As the pure phase information of the incident light is modulated, the image can be reconstructed with high diffraction efficiency [1]. Two factors should be taken into consideration during retrieval of an image: (1) the hologram plane modulates the phase distribution of incident light and maintains its amplitude as unity; (2) only amplitude information is of interest in the image plane. There are various algorithms to compute phase-only holograms, such as the Gerchberg–Saxton (GS) algorithm [2], the Fienup algorithm [3], the Yang–Gu (YG) algorithm [4], the simulated annealing algorithm [5], and the Fienup with do not care method [6].

An electrically controlled phase-only spatial light modulator (SLM) can provide incident light with pixel-by-pixel control of the pure phase in real time [7], just as a dynamic diffractive element, which is widely used in optical micromanipulation [8], optical testing [9], digital holography [10,11], and optical data storage [12]. Much research has been done to calibrate the phase of the SLM using interferometry and then to self-compensate for the phase distortions introduced by the device [13,14]. These methods are effective to adjust the phase of the incident light to improve the image quality of the holographic projection. However, even if the phase hologram is ideally designed, the zero-order intensity exists in the image plane because of the pixelated structure of a phase-only SLM, which is a typical problem when using a commercial SLM for holographic projection of arbitrary light patterns. Several researchers investigated the optical performance of a pixelated SLM. Arrizon *et al.* analyzed the diffraction efficiency produced by the pixelated SLM with a limited fill factor

0003-6935/09/305834-08$15.00/0

and absorbing dead space areas [15]. Palima and Daria modified the model to consider a nonabsorbing dead space, and the modified model allows for derivation of the strength of the zero-order beam at the Fourier plane as a function of the fill factor of a phase-only SLM [16]. More recently, researchers from the same group numerically designed a computer-generated hologram (CGH) that can produce two phases: the desired phase and the corrective phase. The beam with a corrective phase can destructively interfere with the zero-order beam in which the dead space areas are assumed nonabsorbing, and the phases of the dead spaces are assumed to be constant while their amplitude is unity [17]. However, in the actual applications, the modulation in the dead space areas of the pixelated phase-only SLM is more complex. Milewski *et al.* proposed a method in which the zero-order beam is actively removed by forcing some of the light from the active regions of the pixels to fall and destructively interfere with the light resulting from the dead spaces [18]. Nevertheless, this method is computationally demanding and thus typically too slow for real time applications. Here we numerically investigate the influence of the pixelated structure of a SLM on the intensity of a zero-order beam. After two current techniques are reviewed, a new dynamic holographic projection system is proposed. Finally these three approaches are used to eliminate the zero-order beam, and the optical characteristics of the reconstructed image are compared experimentally.

In Section 2 we present the theoretical framework, investigate the impact of all the parameters on the zero-order beam caused by the pixelated structure of the phase-only SLM, and describe in detail the three principles with different loaded phases. We then describe the experimental results in Section 3. Finally, in Section 4 we provide our conclusions.

2. Theory and Methods

A. Optical Characteristic of the Pixelated Phase-Only Spatial Light Modulator

A schematic of the optical system is shown in Fig. 1, in which a phase-only SLM modulates the phase of the incident plane wave and the reconstructed pattern is in the focal plane of the Fourier lens. For simplicity, the GS algorithm is used to retrieve the phase distribution of the hologram plane, which imposes the intensity on the hologram plane as unity and on the image plane as an objective pattern while allowing their phases to switch to an optimum value.

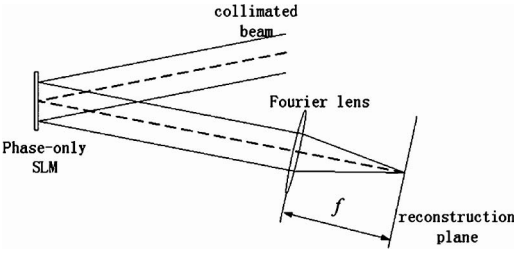

Fig. 1. Basic optical arrangement of the holographic projection system; f is the focal length of the Fourier lens.

We now investigate the modulation of the light field by the pixelated SLM, as shown in Fig. 2. The origin of the *XOY* coordinate system is in the center of the phase-only SLM. The transmittance function of the pixelated SLM can be described as

$$t(x,y) = \mathrm{rect}\left(\frac{x}{L_x},\frac{y}{L_y}\right)\left[t_{\mathrm{ac}}(x,y) + t_{\mathrm{ds}}(x,y)\right], \qquad (1)$$

where the transmittance from the active areas of the SLM is

$$t_{\mathrm{ac}}(x,y) = \mathrm{rect}\left(\frac{x}{a_x},\frac{y}{a_y}\right) \otimes \left\{\frac{1}{d_x d_y}\mathrm{comb}\left(\frac{x}{d_x},\frac{y}{d_y}\right)\exp[i\phi_{\mathrm{ac}}(x,y)]\right\};$$

the transmittance from the dead space areas of the SLM is

$$t_{\mathrm{ds}}(x,y) = \left\{\left[\mathrm{rect}\left(\frac{x}{d_x},\frac{y}{d_y}\right) - \mathrm{rect}\left(\frac{x}{a_x},\frac{y}{a_y}\right)\right] \otimes \frac{1}{d_x d_y}\mathrm{comb}\left(\frac{x}{d_x},\frac{y}{d_y}\right)\right\} A_{\mathrm{ds}}(x,y)\exp[i\phi_{\mathrm{ds}}(x,y)],$$

where L_x and L_y represent the width and the length of the SLM, respectively; $\mathrm{rect}[(x/L_x),(y/L_y)]$ is the aperture function of the SLM; t_{ac} and t_{ds} describe the transmittances from the active areas and the dead space areas of the SLM, respectively; $a_i (i = x,y)$ and $d_i (i = x,y)$ denote the pixel size and the period, respectively; $\otimes$ is the convolution operation; $\phi_{\mathrm{ac}}(x,y)$ is the phase information computed by the GS algorithm, which is loaded on the active areas; and $A_{\mathrm{ds}}(x,y)$ and $\phi_{\mathrm{ds}}(x,y)$ denote the amplitude and the phase modulations of the dead space areas,

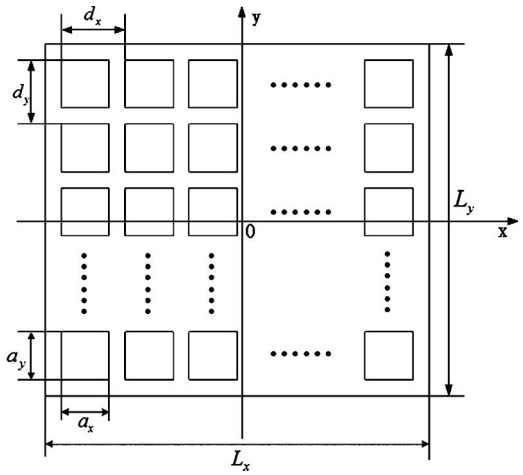

Fig. 2. Geometry of the pixelated phase-only SLM. L_x and L_y represent the width and the length of the SLM, respectively; $a_i (i = x,y)$ and $d_i (i = x,y)$ denote the pixel size and the period, respectively.

respectively. To better analyze the optical transmittance of the pixelated SLM, fill factor μ is defined as

$$\mu = a_x a_y / d_x d_y. \tag{2}$$

The complex amplitude distribution in the reconstruction plane can be calculated as the Fourier transform of $t(x,y)$, that is, $T(f_x,f_y) = \Im[t(x,y)]$, where $\Im$ presents the Fourier transform. By applying the convolution theorem and Fourier transform properties of the comb function, $T(f_x,f_y)$ can be expressed as

$$\begin{aligned} T(f_x,f_y) &= L_x L_y \mathrm{sinc}(f_x L_x, f_y L_y) \\ &\otimes [T_{\mathrm{ac}}(f_x,f_y) + T_{\mathrm{ds}}(f_x,f_y)], \end{aligned} \tag{3}$$

where

$$\begin{aligned} T_{\mathrm{ac}}(f_x,f_y) &= a_x a_y \mathrm{sinc}(f_x a_x, f_y a_y)[\mathrm{comb}(f_x d_x, f_y d_y) \\ &\otimes E(f_x,f_y)], \\ T_{\mathrm{ds}}(f_x,f_y) &= \{[d_x d_y \mathrm{sinc}(f_x d_x, f_y d_y) \\ &\quad - a_x a_y \mathrm{sinc}(f_x a_x, f_y a_y)]\mathrm{comb}(f_x d_x, f_y d_y)\} \\ &\otimes F(f_x,f_y), \end{aligned}$$

$$\begin{aligned} E(f_x,f_y) &= \Im\{\exp[i\phi_{\mathrm{ac}}(x,y)]\}, \\ F(f_x,f_y) &= \Im\{A_{\mathrm{ds}}(x,y)\exp[i\phi_{\mathrm{ds}}(x,y)]\}. \end{aligned}$$

$L_x L_y \mathrm{sinc}(f_x L_x, f_y L_y)$ is a scanning function that approaches the δ function because $L_i (i = x,y)$ is large enough. $T_{\mathrm{ac}}(f_x,f_y) = \Im[t_{\mathrm{ac}}(x,y)]$ describes the contribution from the active areas of the SLM, where the shape of the pixels forms the sinc envelope and the comb function describes the replication of the reconstruction pattern $E(f_x,f_y)$ in the output plane. $T_{\mathrm{ds}}(f_x,f_y) = \Im[t_{\mathrm{ds}}(x,y)]$ describes the contribution from the dead space areas of the SLM. The light distribution in the center of the reconstruction plane (that is, $f_x = f_y = 0$) can be described as

$$\begin{aligned} T(0,0) &= \frac{a_x a_y}{d_x d_y} E(0,0) + \frac{d_x d_y - a_x a_y}{d_x d_y} F(0,0) \\ &= \mu E(0,0) + (1-\mu) F(0,0), \end{aligned} \tag{4}$$

where the first term contains useful information and the second causes zero-order distortion. It is obvious that the three parameters, μ, ϕ_{ds}, and A_{ds}, determine the intensity of the zero-order distortion, and the zero-order distortion monotonically decreases with an increase in μ.

We now investigate the influence of the complex field from the dead space areas on the zero-order distortion caused by the pixelated structure of the SLM. As is well known [18,19], the phase modulation of the light in dead space is adjusted by the voltage loaded on the electrodes of adjacent pixel areas. When the adjacent areas have different settings, there will be a transition area of the phase modulation between the pixel borders because of the LC molecular orientation that gradually changes in the dead space areas. Therefore, to model the discrete phase-only SLM we use linear interpolation with a variable l to describe the phase modulation of the dead space areas, that is,

$$\phi_{\mathrm{ds}}(l) = \phi_{\mathrm{ac}(n)} + l\frac{\phi_{\mathrm{ac}(n+1)} - \phi_{\mathrm{ac}(n)}}{\Delta D}, \qquad l \in (0, \Delta D), \tag{5}$$

where $\phi_{\mathrm{ac}(n)}$ and $\phi_{\mathrm{ac}(n+1)}$ represent the phase modulation from two adjacent pixels of the active areas, and $\Delta D = d_i - a_i (i = x,y)$ is the width of the dead space areas between adjacent pixels. To evaluate the cross ratio of the zero-order optical intensity with that of the image, the relative zero-order intensity in the Fourier plane is defined as

$$\varepsilon = I_0 / \bar{I}, \tag{6}$$

where I_0 is the zero-order intensity of the reconstructed pattern and $\bar{I}$ is the average intensity of the reconstructed pattern.

The amplitude modulation of the light from the dead space varies strongly with the reflection materials. We now numerically simulate the influence of the amplitude modulation of the dead space areas on the zero-order distortion. Figure 3(a) shows the relationship between the relative zero-order intensity ε and A_{ds} with the fill factor $\mu = 83\%$. It is easily observed that, when the fill factor is fixed, ε increases as A_{ds} increases. Figure 3(b) shows the numerically reconstructed pattern when the amplitude modulation of the dead space areas is the same as that of the active areas (that is, $A_{\mathrm{ds}} = 1$). It is evident that the additional zero-order intensity is extremely strong in the center of the reconstructed pattern. It is noted that the totally absorbing dead space areas (that is, $A_{\mathrm{ds}} = 0$) will not result in any additional zero-order intensity, as shown in Fig. 3(c). In brief, the amplitude modulation of the dead space areas determines the relative zero-order intensity for a fixed fill factor.

B. Methods for Eliminating the Zero-Order Beam

Currently there are two methods with which to eliminate the zero-order beam: the spherically loaded phase technique and the linearly loaded phase technique.

1. *Spherically Loaded Phase Technique*

Some researchers try to remove the zero-order noise by separating the imaging data from zero-order illumination along the optical axis [20], as shown in Fig. 4(a), where f is the focal length of the Fourier lens. By adding the phase information of spherical wave ϕ_s to the precalculated phase distribution of the hologram plane, the reconstruction pattern can

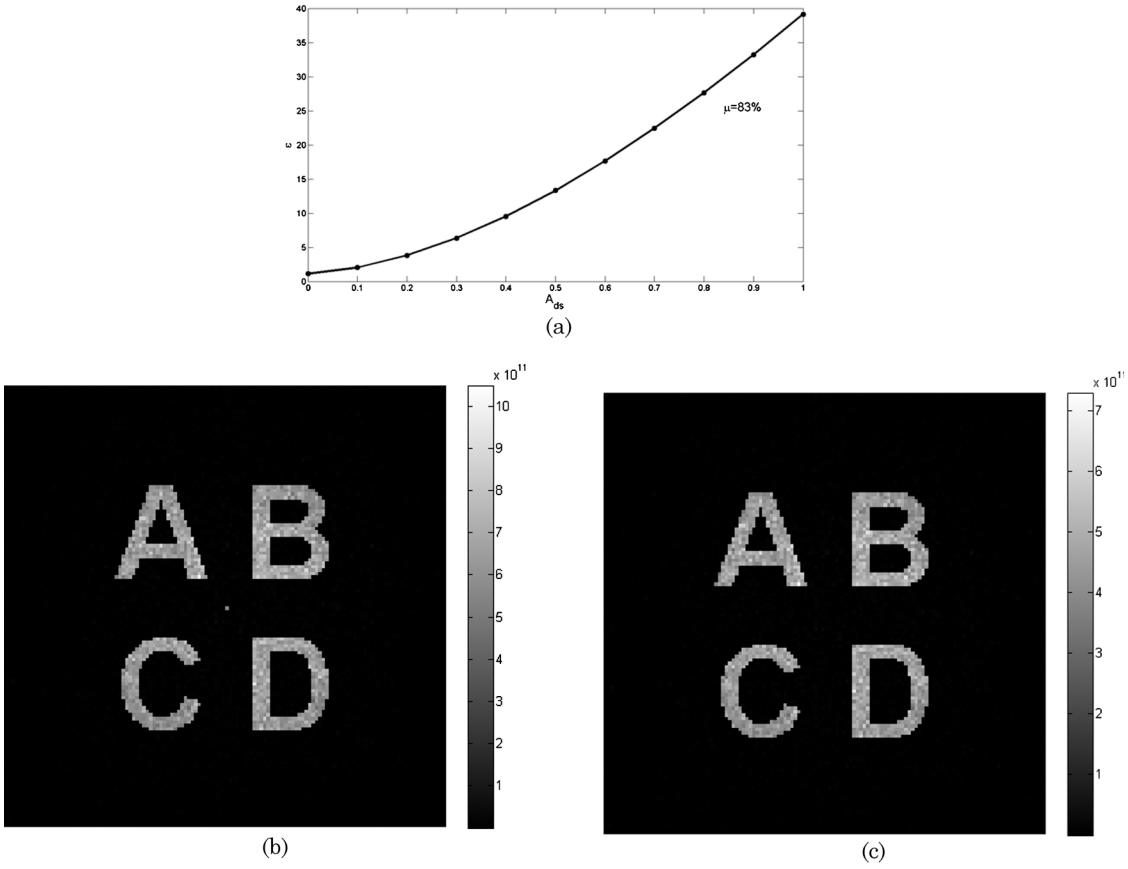

(a) (b) (c)

Fig. 3. (a) Relative zero-order intensity as a function of amplitude modulation of the dead space areas. Numerically reconstructed patterns with (b) $A_{ds} = 1$, $\mu = 83\%$ and (c) $A_{ds} = 0$, $\mu = 83\%$.

be shifted from the focal plane of the Fourier lens and the zero-order illumination would remain unchanged. The phase loaded on the SLM can be expressed as

$$\phi_{SLM} = \phi_{ac} + \phi_s, \tag{7}$$

where ϕ_s denotes the spherically loaded phase. Specifically, an additional convergent spherical wave will lead the reconstruction plane to move closer to the Fourier lens and vice versa. To block the zero-order beam in the light path, the phase information of the divergent spherical wave is chosen to be loaded on the SLM. The phase information of the divergent spherical wave can be calculated as

$$\phi_s(x,y) = \pm\frac{k}{2r}\left(x^2 + y^2\right), \tag{8}$$

where $k = 2\pi/\lambda$ is the wavenumber in free space, λ is the wavelength, r is the distance from the SLM to the center of the divergent spherical wave. The sign on the right-hand side of Eq. (8) is determined by the type of phase-only SLM. If a transmissive SLM is used, there should be a plus sign, and if a reflective one is used there should be a minus sign. The schematic of this technique is shown in Fig. 4(a). The reconstruction plane and the focal plane of the Fourier lens are separated along the optical axis. The distance between the reconstruction plane and the focal plane of the Fourier lens can be expressed as

$$\Delta d = \frac{rf}{r-f}, \tag{9}$$

The real image of the reconstruction pattern can be obtained when $r > f$. The zero-order illumination first forms a spherical wave through the Fourier lens, then focuses in the focal plane of the Fourier lens, and finally spreads out in the reconstruction plane. Since the reconstruction plane is shifted away from the focal plane of the Fourier lens by adding phase information of the divergent spherical wave, the zero-order noise can be blocked by placing a high-pass filter in the focal plane of the Fourier lens. The high-pass filter (normally a transparent glass plate with a predesigned light barrier) should be employed to form a barrier at the focus of the Fourier lens to cancel the zero-order beam, just as shown in Fig. 4(a). Since an additional device is placed in the light path, the quality of the optical reconstruction pattern is slightly degraded.

2. *Linearly Loaded Phase Technique*

In addition to separating the imaging data from zero-order distortion along the optical axis, the

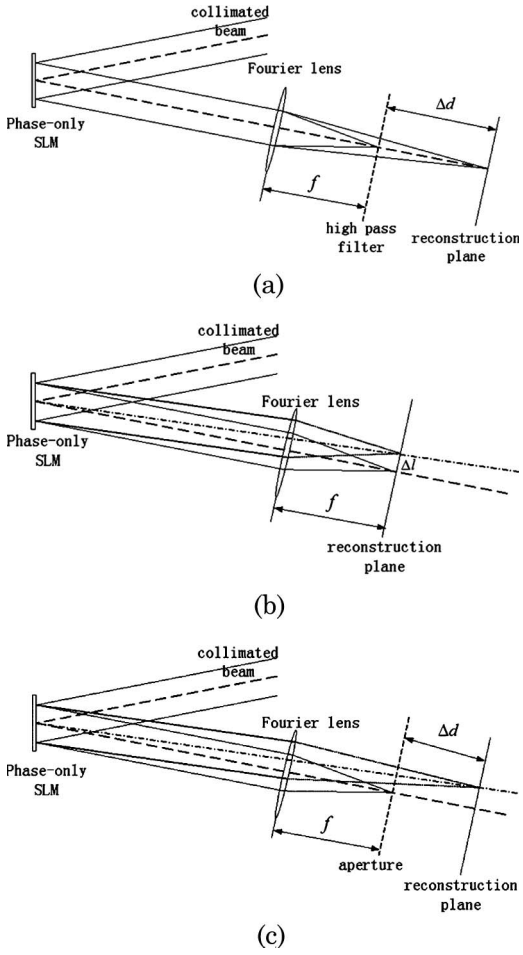

Fig. 4. Optical arrangement for separating the zero-order illumination from the reconstructed pattern by the optimized phase with additional (a) spherically loaded phase, (b) linearly loaded phase, and (c) spherically and linearly loaded phase. Δd is the distance between the reconstruction plane and the focal plane of the Fourier lens. Δl is the distance between the center of the reconstructed pattern and the focus of the Fourier lens.

reconstruction pattern can be moved away from the optical axis by adding an additional linear phase ramp to the precalculated phase [13], where the total phase to be loaded on the SLM can be written as

$$\phi_{\mathrm{SLM}} = \phi_{\mathrm{ac}} + \phi_l, \tag{10}$$

where ϕ_l represents the linearly loaded phase, which can be described as

$$\phi_l(x,y) = (x \sin\beta + y \cos\beta)\tan\theta, \tag{11}$$

θ is the obliquity of the added linear phase ramp, and

$$\beta = \arcsin\left(\frac{x}{\sqrt{x^2+y^2}}\right). \tag{12}$$

Figure 4(b) shows the optical arrangement of the linearly loaded phase technique. The zero-order distortion from the dead space areas is focused to a fixed spot in the focal plane of the Fourier lens. The reconstructed pattern is shifted away from the optical axis because of the additional linear phase ramp loaded on the SLM. The distance between the center of the reconstructed pattern and the focus of the Fourier lens is given by

$$\Delta l = f \tan\theta. \tag{13}$$

It is not necessary to add any filter to the light path, which would simplify the entire system. However, the zero-order illumination and the reconstructed pattern are still in the same plane, which is a limiting factor in the vision system. At the same time, the zero-order beam and the reconstructed pattern interfere with each other. The optical quality of the reconstructed pattern will weaken.

C. Combination of Spherically and Linearly Loaded Phase Technique

Combining the two methods mentioned above, we add both the linear phase and the divergent spherical phase to the precalculated phase distribution on the phase-only SLM, and it is expected that the zero-order illumination and image data can be separated along the optical axis and perpendicular to the optical axis. The phase loaded on the SLM is described as

$$\phi_{\mathrm{SLM}} = \phi_{\mathrm{ac}} + \phi_{\mathrm{sl}}, \tag{14}$$

where ϕ_{sl} is the sum of the divergent spherical phase and linear phases, which can be expressed as

$$\phi_{\mathrm{sl}} = \phi_s + \phi_l. \tag{15}$$

The optical arrangement of this technique is shown in Fig. 4(c). The zero-order illumination focuses on the focal plane of the Fourier lens. The phase of the divergent spherical wave shifts the reconstruction plane further away from the focal plane of the Fourier lens along the optical axis; the linear phase ramp shifts the center of the reconstructed pattern away from the optical axis. The useful information is spatially separated by the zero-order beam in the focal plane of the Fourier lens, and the zero-order beam can be easily blocked by an aperture. Although an aperture is added to the focal plane of the Fourier lens, no optical element affects the reconstruction beam in the light path. Also, the reconstruction plane is not in the focal plane of the Fourier lens, so it can be successfully used in vision systems.

To compare the quality of the reconstructed pattern to the original pattern, we define the signal to noise ratio (SNR) as

$$\mathrm{SNR} = \left\{\frac{\sum_{i=1}^{M}\sum_{j=1}^{N}[O(i,j)]^2}{\sum_{i=1}^{M}\sum_{j=1}^{N}[O(i,j)-R(i,j)]^2}\right\}^{1/2}, \tag{16}$$

where $O(i,j)$ is the desired pattern, $R(i,j)$ is the light distribution of the reconstructed pattern recorded by

the CCD, and M and N are the pixel numbers of the reconstructed and original patterns.

3. Experimental Results

To compare the optical performances of the reconstructed holographic patterns by use of these three phase techniques, we now perform the experiments.

For the experimental work we utilize the *XY* PhaseFlat of liquid crystal on a silicon SLM (Boulder Nonlinear Systems, Lafayette, Colorado, USA), which is a pure phase modulator that consists of 512×512 square pixels, where $L_x = L_y = 7.68\,\text{mm}$, $d_x = d_y = 15\,\mu\text{m}$, $a_x = a_y = 13.70\,\mu\text{m}$, and $\mu = 83.4\%$. The SLM is addressed with 256 gray-scale levels. The wavelength is 632.8 nm and the focal length of the Fourier lens is 500 mm. We used a GP-21400C GigE Vision camera to record the data.

To illuminate the effect of the suppression zero-order beam by the three techniques, we first load the optimized phase on a SLM without an additional loaded phase, and the reconstructed pattern is displayed in Fig. 5(a). It is clear that a strong zero-order beam appears in the center of the reconstructed pattern. To suppress the zero-order beam, we now investigate three different techniques. First, the spherically loaded phase technique is used to eliminate the zero-order beam ($r = 750\,\text{mm}$), and the experimental result is shown in Fig. 5(b). The zero-order beam is blocked by a high-pass filter located in the focal plane of the Fourier lens. It is easily seen that the zero-order beam is suppressed, and the SNR is 1.7302. Second, we investigate the reconstructed pattern with the linearly loaded phase technique; the experimental result is shown in Fig. 5(c) ($\theta = 0.66°$ and $\beta = 90°$). We can see clearly that the imaging data and the zero-order illumination are separated totally, whereas the interference is observed in which the SNR is 1.9285. Finally, we study the reconstructed pattern by our proposed new technique, and the experimental result is displayed in Fig. 5(d). It is evident that the zero-order beam is totally eliminated by adding an aperture to the focal plane of the Fourier lens. The SNR is 2.0112, which is higher than that of others. The utilization efficiency of optical energy of the reconstructed pattern, which is defined as the ratio of total intensity of the reconstructed pattern to the total intensity of the incident light, achieved by the new technique is 28% more than that achieved with the spherically loaded phase technique and almost the same as that achieved with the linearly loaded phase technique.

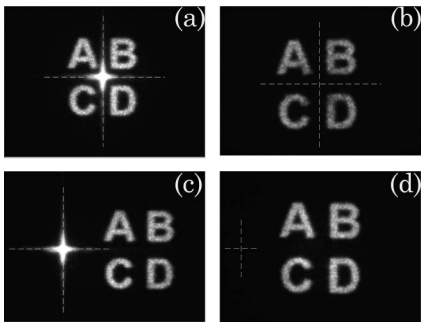

Fig. 5. Output light intensities experimentally detected by a CCD camera for optimized phase (a) without additional loaded phase, (b) with additional spherically loaded phase, (c) with additional linearly loaded phase, (d) with additional spherically and linearly loaded phase. (The intersections of the dashed lines indicate the optical axis).

The quality of the reconstructed pattern by use of the spherically loaded phase technique is poorer than that of the others because the high-pass filter affects the reconstruction quality, and the transparency of the plate and the light block of the high-pass filter reduce the diffraction efficiency of the entire system. In addition, the nonideal planeness of the transparent plate weakens the image quality of the reconstruction pattern because of the additional fluctuation in phase information. The new technique uses an aperture to block the zero-order beam, which will not affect the reconstruction beam in the light path. The experimental results show that our technique can achieve better reconstruction quality and diffraction efficiency.

To further illuminate the availability of our technique to eliminate the zero-order beam *in vivo*, we show a short animated movie for dynamic holographic projection, and one frame of it is shown in Fig. 6 (Media 1). It can be clearly seen that our technique can eliminate the zero-order beam successfully in a dynamic holographic projection system.

4. Discussion and Conclusion

The phase modulation of the incident light loaded by the SLM is discrete, so the phases ϕ_s, ϕ_l, and ϕ_{sl} are added to the precalculated phase distribution on the hologram plane. Each technique uses a space–bandwidth product (SBP) of the SLM to adjust the location of the zero-order beam, so that the SLM SBP will be reduced in the image plane. This procedure is crucial to investigate the effect of the spatial frequency of the added phase information on the quality of the image.

Now we analyze the effect of linearly loaded phase ϕ_l on the image. For the linearly loaded phase technique, $\exp(i\phi_{\text{SLM}}) = \exp[i(\phi_{\text{ac}} + \phi_l)] = \exp(i\phi_{\text{ac}})$

Fig. 6. Single-frame excerpts from the video produced by holographic projection (Media 1).

$\exp(i\phi_l)$, this indicates that the spatial frequency spectrum of ϕ_{ac} is convoluted with that of ϕ_l in the image plane. We set ξ and η as the coordinate system of the image plane. The spatial frequency spectrum of ϕ_l on the ξ axis direction is shown in Fig. 7 (solid line), and it is obvious that it is an impulse function. As θ increases, the pulse position moves laterally. Also, the pulse width will gradually expand because of the discrete expression of ϕ_l, as shown in Fig. 8(a) (solid line). Because the frequency is $f_\xi \in [-1/2d_x, 1/2d_x]$ and $\sin\theta = f_\xi\lambda$, the maximum of θ is 1.21°. The dashed line in Fig. 7 represents the spatial frequency spectrum of ϕ_l on the ξ axis when $\theta = 0.66°$, from which we can clearly see the increase in bandwidth.

A similar procedure can be used to analyze the effect of the spherically loaded phase ϕ_s on the image quality, as shown in Fig. 8(b). Because the focal length of the Fourier lens is 500 mm, r should be larger than 500 mm to achieve a real image in the image plane. The dotted line in Fig. 7 represents the frequency spectrum of ϕ_s on the ξ axis when $r = 750$ mm, which is almost the same as that of $\theta = 0°$ in the case of the linearly loaded phase technique. The spatial frequency bandwidth is extremely narrow in the image plane as can be seen in Fig. 8(b) (solid line). So when we load phase ϕ_{sl}, the effect of the spherically loaded phase is trivial, as shown in Fig. 8(a) (dotted line). The dash–dot line in Fig. 7 shows the frequency spectrum of ϕ_{sl} on the ξ axis when $r = 750$ mm and $\theta = 0.66°$, and there is almost no difference in comparison with the dashed line in Fig. 7. Theoretically, the expansion of the frequency bandwidth will degrade the quality of the reconstructed image. However, from the above experimental results we can see that the effect is negligible in comparison with the noise induced by the optical system.

In brief, we analyzed the influence of the pixelated structure of the phase-only SLM on zero-order interruption in holographic projection. The optical field distribution in the focal plane of the Fourier lens can be divided into two parts: the optical field distribution diffracted by the active areas which is useful and the additional zero-order optical field distribution contributed by the dead space areas. The simulation results show that the relative zero-order intensity depends on the amplitude modulation of the dead space area and the fill factor of the pixelated phase-only SLM. A new technique has been proposed to eliminate the zero-order beam by adding both a linear phase and a divergent spherical phase to the precalculated phase distribution on the phase-only SLM. In comparison with the two currently existing techniques, our technique can achieve a reconstructed holographic pattern with higher diffraction efficiency and better optical contrast and quality. Experimental results show that it is an efficient technique for elimination of the zero-order beam in vision systems. This technique can also be used to eliminate the zero-order interruption in optical systems based on pixelated phase-only SLMs.

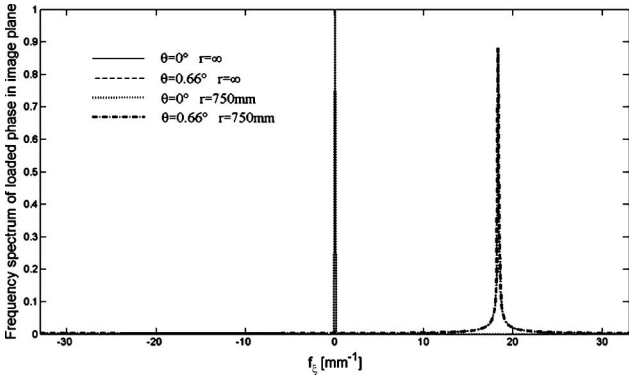

Fig. 7. Spatial frequency spectrum on the ξ axis in the image plane.

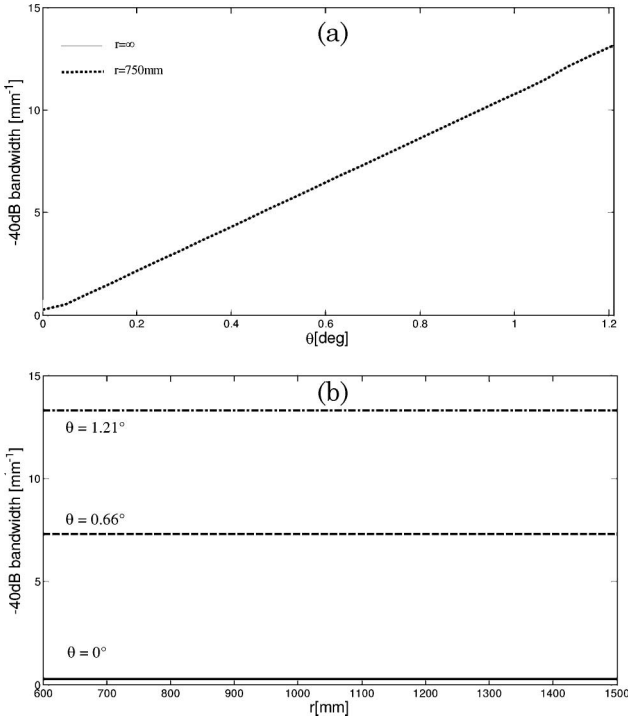

Fig. 8. Spatial frequency with a −40 dB bandwidth as a function of (a) θ of the linearly loaded phase when $r = \infty$ and $r = 750$ mm, (b) r of the spherically loaded phase when $\theta = 0°$, $\theta = 0.66°$, and $\theta = 1.21°$.

This research was supported by the Innovation Team Development Program of the Chinese Ministry of Education, grant IRT0606, and the National Basic Research Program of China, grant 2006CB302901.

References

1. H. Dammann and K. Gortler, "High-efficiency in-line multiple imaging by means of multiple phase holograms," Opt. Commun. **3**, 312–315 (1971).
2. R. W. Gerchberg and W. O. Saxton, "A practical algorithm for the determination of phase from image and diffraction plane pictures," Optik (Jena) **35**, 237–246 (1972).
3. J. R. Fienup, "Reconstruction of an object from the modulus of its Fourier transform," Opt. Lett. **3**, 27–29 (1978).

4. B. Gu, G. Yang, and B. Dong, "General theory for performing an optical transform," Appl. Opt. **25**, 3197–3206 (1986).
5. S. Kirkpatrick, C. D. Gelatt, Jr., and M. P. Vecchi, "Optimization by simulated annealing," Science **220**, 671–680 (1983).
6. A. Georgiou, J. Christmas, N. Collings, J. Moore, and W. A. Crossland, "Aspects of hologram calculation for video frames," J. Opt. A Pure Appl. Opt. **10**, 035302 (2008).
7. A. Georgiou, J. Christmas, J. Moore, A. Jeziorska-Chapman, A. Davey, N. Collings, and W. A. Crossland, "Liquid crystal over silicon device characteristics for holographic projection of high-definition television images," Appl. Opt. **47**, 4793–4803 (2008).
8. H. Melville, G. Milne, G. Spalding, W. Sibbett, K. Dholakia, and D. McGloin, "Optical trapping of three-dimensional structures using dynamic holograms," Opt. Express **11**, 3562–3567 (2003).
9. Z. Cao, L. Xuan, L. Hu, Y. Liu, Q. Mu, and D. Li, "Investigation of optical testing with a phase-only liquid crystal spatial light modulator," Opt. Express **13**, 1059–1065 (2005).
10. A. Michalkiewicz, M. Kujawinska, J. Kretzel, L. Salbut, X. Wang, and P. J. Bos, "Phase manipulation and optoelectronic reconstruction of digital holograms by means of LCOS spatial light modulator," Proc. SPIE **5776**, 144–152 (2005).
11. C. Kohler, X. Schwab, and W. Osten, "Optimally tuned spatial light modulators for digital holography," Appl. Opt. **45**, 960–967 (2006).
12. J. Joseph and D. A. Waldman, "Homogenized Fourier transform holographic data storage using phase spatial light modulators and methods for recovery of data from the phase image," Appl. Opt. **45**, 6374–6380 (2006).
13. X. Xun and R. W. Cohn, "Phase calibration of spatially nonuniform spatial light modulators," Appl. Opt. **43**, 6400–6406 (2004).
14. J. Otón, P. Ambs, M. S. Millán, and E. Pérez-Cabré, "Multipoint phase calibration for improved compensation of inherent wavefront distortion in parallel aligned liquid crystal on silicon displays," Appl. Opt. **46**, 5667–5679 (2007).
15. V. Arrizon, E. Carreon, and M. Testorf, "Implementation of Fourier array illuminators using pixelated SLM: efficiency limitations," Opt. Commun. **160**, 207–213 (1999).
16. D. Palima and V. R. Daria, "Effect of spurious diffraction orders in arbitrary multifoci patterns produced via phase-only holograms," Appl. Opt. **45**, 6689–6693 (2006).
17. D. Palima and V. R. Daria, "Holographic projection of arbitrary light patterns with a suppressed zero-order beam," Appl. Opt. **46**, 4197–4201 (2007).
18. G. Milewski, D. Engström, and J. Bengtsson, "Diffractive optical elements designed for highly precise far-field generation in the presence of artifacts typical for pixelated spatial light modulators," Appl. Opt. **46**, 95–105 (2007).
19. M. Gruneisen, L. DeSandre, J. Rotge, R. Dymale, and D. Lubin, "Programmable diffractive optics for wide-dynamic-range wavefront control using liquid-crystal spatial light modulators," Opt. Eng. **43**, 1387–1393 (2004).
20. J. Christmas, N. Collings, A. Georgiou, "Blocking zero-order in phase shift hologram generation," UK patent GB2438458 (28 November 2007).